JOURNAL OF GUIDANCE, CONTROL, AND DYNAMICS
Vol. 18, No. 5, September–October 1995

Feedback System Design for Stable Plants with Input Saturation

R. A. Hess*
University of California, Davis, Davis, California 95616

Most, if not all, flight control systems are subject to saturation nonlinearities such as amplitude limiting. These are often referred to as nuisance nonlinearities, existing as they do in almost all designs. However, when such saturations do occur, flight control system performance can be degraded considerably. A technique is presented that can allow the performance of a multi-input, multi-output control system design with stable plants to be improved when operating in the presence of saturating nonlinearities. The technique is an extension of that previously discussed in the literature with regard to single-input, single-output systems. An example of the design technique is presented dealing with a longitudinal autopilot design of a simple rotorcraft model, wherein command limiting in the airspeed and altitude command modes is encountered.

Nomenclature

h = altitude perturbation, ft
q = pitch rate, rad/s
t^{pi} = instant of pth switch of output of n_i from linear to nonlinear mode
t_{pi} = instant of pth switch of output of n_i from nonlinear to linear mode
u = x body axis component of perturbed velocity, ft/s
w = z body axis component of perturbed velocity, ft/s
δ_B = longitudinal cyclic, deg swashplate
δ_C = collective, deg swashplate
θ = pitch attitude, rad

Introduction and Background

SATURATION nonlinearities are present in any flight control system. These nonlinearities can be particularly troublesome since they are not amenable to treatment by most nonlinear control system design techniques, e.g., nonlinear quantitative feedback theory[1] and nonlinear inversion techniques.[2] Progress has been made in designing systems that explicitly consider these saturation characteristics from the outset.[3,4] This approach requires a supervisory control loop that modifies the system error signals so that saturation does not occur. Although attractive from a number of standpoints, particularly in its applicability to unstable plants, the control structures associated with this approach can be quite complicated.

The control system design technique to be discussed here builds upon a formulation introduced by Horowitz.[1,5,6] In single-input, single-output (SISO) systems, Horowitz showed that one could achieve independent loop transmissions with respect to the plant and the saturating nonlinearity. This was accomplished with the addition of a feedback loop around the nonlinearity, assuming that the appropriate sensing requirements could be met. Horowitz showed that the additional degree of freedom provided by the independent loop transmission around the nonlinear element could be exploited to improve system performance when saturation occurred. As opposed to the technique of Refs. 3 and 4, the design technique offered by Horowitz begins with the linear control system design, e.g., compensator and prefilter, which achieved desired linear system performance in the presence of plant uncertainty. The elements of Horowitz's approach will be retained in the extension to a multi-input, multi-output (MIMO) system as described in the following section. Application of the design technique will be limited to stable plants in this discussion, where a stable plant is defined as having all poles in the left-half plane but allowing poles at the origin.

Received May 16, 1994; revision received Dec. 18, 1994; accepted for publication Feb. 17, 1995.
*Professor, Department of Mechanical and Aeronautical Engineering. Associate Fellow AIAA.

Design Technique

Problem Formulation

Consider the MIMO control system shown in Fig. 1a. Here, the quantities $\boldsymbol{r}$, $\boldsymbol{x}$, $\boldsymbol{y}$, and $\boldsymbol{c}$ are vector quantities and $\boldsymbol{F}$, $\boldsymbol{G}$, $\boldsymbol{N}$, and $\boldsymbol{P}$ represent matrices. Figure 1b represents the nonlinear saturation characteristics n_i, $i = 1, \ldots, m$, where m is the number of rows of $\boldsymbol{G}$ (and columns of $\boldsymbol{P}$). Fundamental to the technique to be described is the fact that $\boldsymbol{F}$ and $\boldsymbol{G}$ have been obtained by a suitable design procedure for linear systems.

Input–Output Relations

Let us consider the input x_i to the ith nonlinearity n_i. This can be expressed as

$$x_i = \sum_{j=1}^{n_r} T_{x_i r_j} r_j + T_{x_i y_i} y_i + \sum_{\substack{j=1 \\ j\neq i}}^{n_y} T_{x_i y_j} y_j \qquad i = 1, \ldots, n_y \quad (1)$$

where n_r and n_y are the number of inputs and nonlinear element outputs, respectively. Here, the T_{xr} and T_{xy} elements represent linear transfer functions $x(s)/r(s)$ and $x(s)/y(s)$ obtained with the r and x treated as controlled sources.[1] Next consider that the ith nonlinearity shown in Fig. 1b has been replaced by unity, i.e., $y_i(s)/x_i(s) = 1.0$ and $y_i(t) \equiv y_{i_L}(t)$. One can write

$$x_{i_L} = \sum_{j=1}^{n_r} T_{x_i r_j} r_j + T_{x_i y_i} y_{i_L} + \sum_{\substack{j=1 \\ j\neq i}}^{n_y} T_{x_i y_j} y_j \quad (2)$$

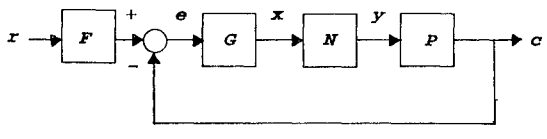

Fig. 1a MIMO control system with nonlinearities.

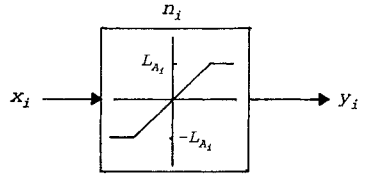

Fig. 1b Saturating nonlinearity.

Thus, the subscript L in Eq. (2) refers to the fact that the ith nonlinear element has been replaced by unity. In Eq. (2) it has been assumed that all of the remaining nonlinearities n_k, $k = 1, \ldots, n_y$, $k \neq i$, are still present. The validity of this equation is maintained despite the presence of nonlinearities n_k by the retention of the $y_j(s)$, which are the transforms of output of the n_k nonlinear elements, i.e., the $y_j(s)$ represent controlled sources.

Considering the $2n_y$ equations implied by Eqs. (1) and (2) and taking them in pairs, i.e., $i = 1$ in Eqs. (1) and (2), then $i = 2, \ldots,$ and one can show

$$x_i - y_i = (y_{i_L} - y_i)(1 - T_{x_i y_i}) \tag{3}$$

Equation (3) can be obtained as follows. With $i = 1$, solve Eq. (2) for $T_{x_1 r_j}$. Substitute the resulting expression for $T_{x_1 r_j}$ into Eq. (1), and subtract y_1 from both sides of the relation. Now define

$$L_{n_i} \triangleq -T_{x_i y_i} \qquad \text{and} \qquad \Delta_i \triangleq x_i - y_i \tag{4}$$

where L_{n_i} represents the loop transmission around the nonlinearity n_i. This gives

$$\Delta_i = (y_{i_L} - y_i)(1 + L_{n_i}) \tag{5}$$

Now if all the nonlinearities were replaced by unity, one would have $\Delta_i = 0, i = 1, \ldots, n_y$. In the SISO case, Eq. (5) is useful for determining the behavior of the outputs of the nonlinear elements n_i when they emerge from saturation.[1,5,6]

Nonlinear Element Output Behavior

Let us consider that only one of the elements of N (call it n_i) is nonlinear, i.e., it possesses the characteristics shown in Fig. 1b. Further, assume that the amplitude limits L_{A_i} are each unity. Nonunity values can be handled easily through appropriate normalizations.[1,5,6] With t^{pi} and t_{pi} defined in the Nomenclature:

$$y_{pi}(t) = \begin{cases} y(t) & t < t_{pi} \\ 0 & t \geq t_{pi} \end{cases} \qquad y^{pi}(t) = \begin{cases} 0 & t < t_{pi} \\ y(t) & t \geq t_{pi} \end{cases}$$

In the discussions to follow, it will be assumed that the system is quiescent for $t < 0$ and that $t^{pi} < t_{pi}$, i.e., the system begins with linear behavior.

With the definitions just given, it can be shown[1,5,6] that Eq. (3) becomes

$$(y_i(s))^{pi} - (y_{i_L}(s))^{pi} = (\Delta_i(s))^{pi} + \frac{\{L_{n_i}[(y_{i_L}(s))_{pi} - (y_i(s))_{pi}]\}^{pi}}{1 + L_{n_i}} \tag{6}$$

where $(y_i(s))^{pi}$ is the Laplace transform of $(y_i)^{pi}(t)$. The numerator of the last term on the right-hand side deserves some explanation. It represents the Laplace transform of

$$\left\{ \int_0^t l_{n_i}(\tau)[(y_{i_L})_{pi}(t - \tau) - (y_i)_{pi}(t - \tau)]\, d\tau \right\}^{pi} \tag{7}$$

One can now examine the behavior of the system if saturation occurs. Figure 2 demonstrates a possible scenario. Here transient inputs $r_j(t)$ are assumed to have been applied. By transient is meant that $r_j(t) \to 0$ as $t \to \infty$. It should be noted that it is inconsequential whether y_{i_L} is due to inputs, disturbances, or a combination of the two.[1] Further assume that n_i amplitude saturates from t^{1i} to t_{1i}. This is shown in Fig. 2 for the original design. Consider the implications of Eq. (6) when an independent L_{n_i} is available. For reasons that will be obvious in what follows, choose $L_{n_i} \approx K_i/s$. Now, for $p = 1$, $t \geq t_{1i}$, and with $(\Delta_i(s))^{1i} = 0$ by definition, Eq. (6) yields

$$\left[\left(1 + \frac{K_i}{s}\right)[(y_i(s))^{1i} - (y_{i_L}(s))^{1i}] \right]$$

$$= \left\{ e^{-t_{1i}s} K_i \mathcal{L}\left[\int_0^t [(y_{i_L})_{1i}(t - \tau) - (y_i)_{1i}(t - \tau)]\, d\tau \right] \right\}^{1i} \tag{8}$$

where $\mathcal{L}[\cdot]$ denotes the Laplace transform of $[\cdot]$. The integral on the right-hand side of Eq. (8) can be seen to be the area A_1–A_2 in Fig. 2. Thus, in the time domain, Eq. (8) states

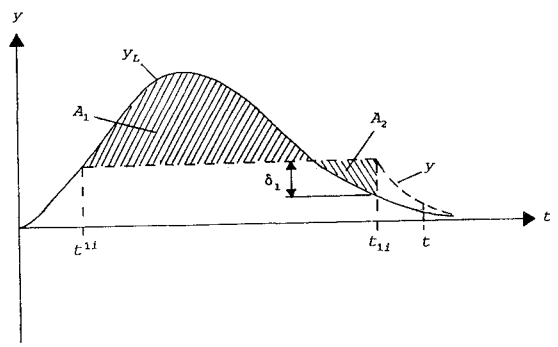

Fig. 2 Nonlinear and linear system behavior, $L_{n_i} \approx K_i/s$.

$$(y_i)^{1i}(t) - (y_{i_L})^{1i}(t) = K_1(A_1 - A_2)e^{-K_1(t - t_{1i})}u(t - t_{1i})$$

$$= \delta_1 e^{-K_1(t - t_{1i})}u(t - t_{1i}) \tag{9}$$

Note, at $t = t_{1i}$, that

$$(y_i)^{1i}(t_{1i}) - (y_{i_L})^{1i}(t_{1i}) = K_1(A_1 - A_2) = \delta_1 \tag{10}$$

Thus t_{1i} could be found from the time histories of Fig. 2.

Equation (9) is valid until the next saturation occurs in the output of element n_i. Equation (9) demonstrates an important result. In every time interval after y_i comes out of saturation, y_i will approach y_{i_L} with dynamics $(1 + L_{n_i})^{-1}$, i.e., exponentially in the time domain. This is indicated in Fig. 2. The rationale for choosing $L_{n_i} \approx K_i/s$ is now evident. Since this is the first nonlinearity considered, y_{i_L} is the y_i that exists in the completely linear system, which has been designed to be stable. The idea here is to have the dynamics $(1 + L_{n_i})^{-1}$ be fast as compared to the dynamics of y_i. Of course, the means of accomplishing this is with the magnitude of K_i. The analysis just completed requires that y_i does not remain in saturation if saturation occurs. It does not guarantee that y_i will come out of saturation. Conditions sufficient for eliminating the possibility of steady-state saturation of y_i will be assumed to met here and will be discussed in a later section.

The reader should be cautioned that, although an intuitively attractive result, the actual system performance improvements associated with y_i approaching y_L quickly are not quantitatively defined and can depend upon the plant dynamics.[1]

We can next move on to the next nonlinear element, n_k, while retaining the nonlinear n_i. The analysis just described can be repeated. Once again, Eqs. (3–9) apply. Equation (9) says that in every interval after element y_k comes out of saturation, y_k will approach y_{k_L} with dynamics $(1 + L_{n_k})^{-1}$. However, since a nonlinear element is involved (the n_i from the first design), the linear y_{k_L} refers to the behavior of the element n_k when no saturation occurs in that element alone. Conceptually, one can proceed through the system, forming loop transmissions L_{n_i} around each nonlinearity. The analysis just described guarantees behavior described by Eq. (9) if the y_i come out of saturation.

Recall the assertion that the required L_{n_i}, the loop transmission about n_i, has been created independently of any loop transmissions about the plant. A means of accomplishing this for MIMO systems will now be presented.

Creating Independent Loop Transmissions

Perhaps the best way to demonstrate how one can choose independent loop transmissions about nonlinear elements and the plant is by the simple 2×2 example shown in Fig. 3a. The system with prefilter and compensator elements f_i and g_{ij} and plant elements p_{ij} has been created with some linear MIMO control design technique. Consider Fig. 3b, wherein two feedback loops with compensation h_1 and h_2 have been added around n_1 and n_2, respectively, and the compensation elements $g_{11} \to g_{22}$ have been modified to $g'_{11} \to g'_{22}$. For linear operation (no saturations occurring), Fig. 3b can be made equivalent to Fig. 3a. From Fig. 3b, one can easily show the following:

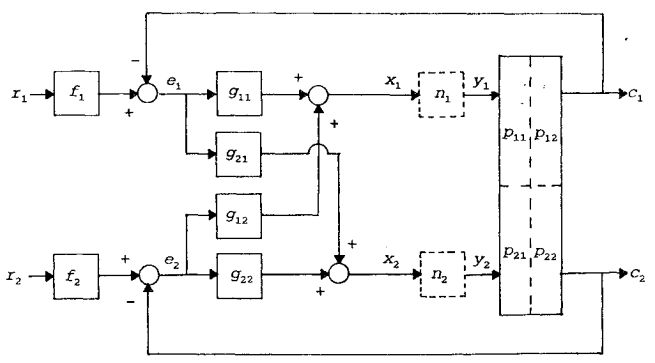

Fig. 3a 2 × 2 MIMO control system with nonlinearities.

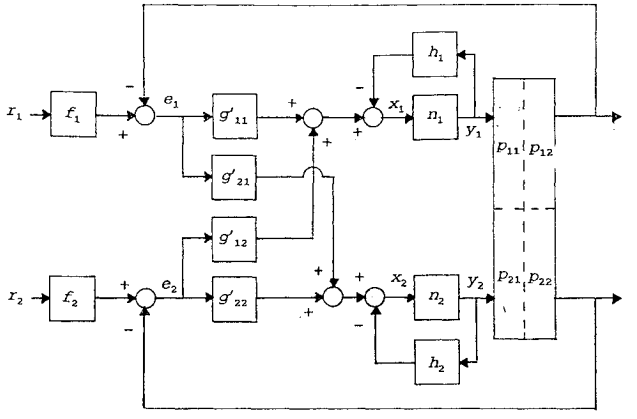

Fig. 3b Nonlinear design with independent loop transmissions.

Loop around n_1:

$$L_{n_1} \triangleq -T_{x_1 y_1} = p_{11}(g'_{11}) + p_{21}(g'_{12}) + h_1 \tag{11a}$$

Loop around n_2:

$$L_{n_2} \triangleq -T_{x_2 y_2} = p_{22}(g'_{22}) + p_{12}(g'_{21}) + h_2 \tag{11b}$$

and

$$\begin{aligned} L_{11} &\triangleq T_{c_1 e_1} = p_{11}\frac{g'_{11}}{1+h_1} + p_{12}\frac{g'_{21}}{1+h_2} \\ L_{22} &\triangleq T_{c_2 e_2} = p_{21}\frac{g'_{12}}{1+h_1} + p_{22}\frac{g'_{22}}{1+h_2} \\ L_{21} &\triangleq T_{c_2 e_1} = p_{21}\frac{g'_{11}}{1+h_1} + p_{22}\frac{g'_{21}}{1+h_2} \\ L_{12} &\triangleq T_{c_1 e_2} = p_{11}\frac{g'_{12}}{1+h_1} + p_{12}\frac{g'_{22}}{1+h_2} \end{aligned} \tag{11c}$$

The last four relations are computed assuming $n_1 = n_2 = 1.0$. The first two of Eqs. (11) can be expressed in matrix form as $\boldsymbol{L}_n = [\boldsymbol{G'P}]_d + \boldsymbol{H}$, where $\boldsymbol{L}_n$ and $\boldsymbol{H}$ are diagonal matrices with elements L_{n_i} and h_i along the diagonal and $[\cdot]_d$ indicates a diagonal matrix formed by setting the off-diagonal elements of $[\cdot]$ equal to zero. The last four equations can be expressed as $\boldsymbol{L} = \boldsymbol{PJG'}$, where $\boldsymbol{J}$ is defined as

$$\boldsymbol{J} \triangleq \begin{bmatrix} \dfrac{1}{1+h_1} & 0 \\ 0 & \dfrac{1}{1+h_2} \end{bmatrix} \tag{12}$$

Note that $\boldsymbol{J}^{-1} = \boldsymbol{I} + \boldsymbol{H}$. The relations in Eqs. (11) offer six equations in the six unknowns g'_{ij} and h_i, $i, j = 1, 2$. The knowns are L_{ij}, L_{n_i}, and the nominal plant elements p_{ij}. The L_{ij} can, of course, be determined from the g_{ij} and the nominal plant elements p_{ij}. Thus, the L_{n_i} can be chosen independently of the L_{ij}. For square nonsingular $\boldsymbol{P}$, the task of solving for the unknowns can be made more systematic by considering the matrix relations

$$\boldsymbol{L} = \boldsymbol{PJG'} \tag{13}$$

or

$$\boldsymbol{G'} = \boldsymbol{J}^{-1}\boldsymbol{P}^{-1}\boldsymbol{L} = [\boldsymbol{I} + \boldsymbol{H}]\boldsymbol{P}^{-1}\boldsymbol{L} \tag{14}$$

Rewriting a previous result

$$\boldsymbol{H} = (\boldsymbol{L}_n - [\boldsymbol{G'P}]_d) \tag{15}$$

One has

$$\boldsymbol{G'} = (\boldsymbol{I} + \boldsymbol{L}_n - [\boldsymbol{G'P}]_d)\boldsymbol{P}^{-1}\boldsymbol{L} \tag{16}$$

Equation (16) now offers a set of linear algebraic equations in the unknowns g'_{ij} that can be found and substituted into Eq. (15) to find the h_i.

Stability Considerations

The preceding section has discussed, in very general terms, a design technique that appears to have the potential of improving the performance of systems subject to saturation. The asserted improvement lies in the fact that, if and when coming out of saturation, the output of each nonlinearity exponentially approaches the output that would be in evidence if no saturation existed in that nonlinearity. If the system operates entirely in a linear mode (no saturation occurs at any time), the system dynamics are identical to those of the original linear design, e.g., those of Fig. 3a. Of course, performance improvement is moot if closed-loop stability cannot be maintained.

Stability for SISO Systems

The sufficient conditions for stable behavior for SISO systems are the creation of $L_n = K/s$ and internal stability and no steady-state saturation.

Internal Stability. Reference 7 presents a discussion showing that a stable plant (all poles in the left-half plane, but allowing poles at the origin) is a sufficient condition for internal stability of $g'/(1+h)$.

No Steady-State Saturation. Plant dynamics of at least type 1 ensures that the nonlinear element will come out of saturation, again assuming a transient input.

Stability for MIMO Systems

Using the simple system of Fig. 3a as an example, one can use Eqs. (11) to determine h_i and g'_{ij}, resulting in Fig. 3b, with desired L_{n_i}. The question then is to determine the sufficient conditions for stability. First, internal stability and no steady-state saturation are required.

Internal Stability. With the present formulation, a necessary condition for internal stability will be a stable plant, as defined in the preceding. Thus, it will be assumed that the plant $\boldsymbol{P}$ of Fig. 3 is stable. The plant $\boldsymbol{P}$ may indeed be an effective plant, modified by feedback closures not explicitly shown in the figure. However, as opposed to the SISO case, it may still be possible for the individual compensation elements g'_{ij}, h_i, and $1/(1+h_i)$ to exhibit unstable poles. Techniques for assuring stable elements are under investigation, and it will be assumed herein that stable elements are in evidence.

No Steady-State Saturation. Conditions that are sufficient for ensuring that nonlinear elements do not remain in saturation are a generalization of the plant type restriction for SISO systems. Referring to Eq. (1), to bring y_i out of saturation when y_i and any or all of the remaining y_j go into saturation, one needs to have

$$\lim_{s \to 0} x_i(s) \propto -\frac{\text{sgn(saturated } y_i)}{s^{p+1}} \qquad p \geq 1 \tag{17}$$

Relation (17) essentially forces the steady-state input to the nonlinearity n_i to be the negative of the pth integral of the saturated output value, hence providing a sufficient condition that the output will

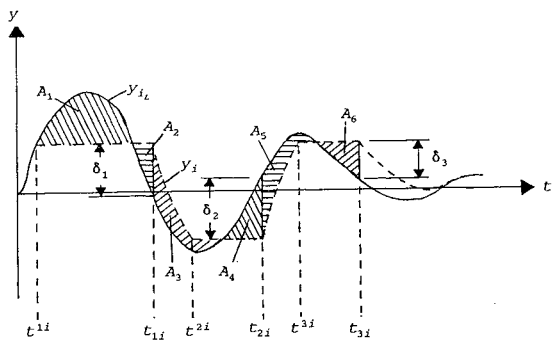

Fig. 4 Nonlinear and linear system behavior; stability with $L_{n_i} \approx K_i/s$.

eventually come out of saturation. The loop transmissions around each nonlinearity have been forced to be

$$L_{n_i} \triangleq -T_{x_i y_i} = \frac{K_i}{s} \tag{18}$$

Thus, considering the Laplace transform of Eq. (1) with y_i and y_j assigned their limiting values $\pm L_{A_i}$ and $\pm L_{A_j}$ (Fig. 1), one has

$$x_i(0) = \sum_{j=1}^{n_r} T_{x_i r_j}(0) r_j(0) - \frac{K_i}{s}\left[\frac{\pm L_{A_i}}{s}\right] + \sum_{\substack{j=1 \\ j \neq i}}^{n_y} T_{x_i y_j}(0)\left[\frac{\pm L_{a_j}}{s}\right] \tag{19}$$

With SISO systems, it can be shown that relations (17) and (19) lead to the requirement that the plant be of at least type 1. In the MIMO case, it is much more difficult to interpret these relations in terms of plant characteristics. However, after completing the design, one can evaluate the right-hand side of Eq. (19) with all possible combinations of limiting values.

It will now be demonstrated that stability will be ensured for MIMO systems with $L_{n_i} = K_i/s$, internal stability, and no steady-state saturation. The system of Fig. 3b will be used for the purposes of exposition. The proof to be presented borrows heavily on that presented by Horowitz for SISO systems.[1,5,6]

Consider Fig. 4, which shows hypothesized behavior of the signals $y_i(t)$ and $y_{i_L}(t)$ to transient inputs or disturbances. Here let $i = 1$. By definition, signal $y_{1_L}(t)$ is that which would exist if $n_1 = 1$. Assume that $y_{1_L}(t) \to 0$ as $t \to \infty$, as shown. As indicated by Eq. (10), the sign convention for the δ_i is that a positive δ_i indicates that $y_i > y_{i_L}$ when y_i comes out of saturation. As opposed to the $y_L(t)$ in Fig. 2, the $y_{1_L}(t)$ in Fig. 4 has been shown to be oscillatory so as to allow $y_1(t)$ to resaturate. Now only $y_{1_L}(t)$ and L_{n_1} are needed to find the alternating linear and saturation intervals. In a manner similar to that exploited in Fig. 2, the t_{pi} ($p = 1, 2, 3$, $i = 1$) in Fig. 4 are obtained as follows:

$$\begin{aligned} t_{11}&: \quad A_1 - A_2 = \delta_1/K_1 \\ t_{21}&: \quad A_3 - A_4 = (\delta_1 + \delta_2)/K_1 \\ t_{31}&: \quad A_5 - A_6 = (\delta_2 + \delta_3)/K_1 \end{aligned} \tag{20}$$

The first saturation point t^{11} is the first instant $y_{11} = 1.0$. Any other t^{p1} is obtained from Eq. (6) by first convolving $(y_{1_L})_{p1}(t) - (y_1)_{p1}(t)$ with $l_{n_1}(t)$ over the shifted time $t - t_{p1}$. With this convolution defined as $z_{p1}(t)$, one finds

$$\mathcal{L}^{-1}\left[z_{p1}(s)\frac{s}{s+K_1}\right] \triangleq (y_1(s))^{p1} - (y_{1_L}(s))^{p1} \tag{21}$$

with $L_{n_1} = K_1/s$; z_{p1} is simply $K_1(A_1 - A_2) = \delta_1$. So, for $p = 2$

$$(y_1)^{21}(t) = (y_{1_L})^{21}(t) + \delta_1 e^{-K_1(t-t_{21})}u(t - t_{21}) \tag{22}$$

This process continues for finding other t^{p1}. Eventually, a time t_s will be reached wherein $|y_{1_L}(t)| < L_{A_1}$ (here assumed to be unity) for $t \geq t_s$. For the next $t_{p1} > t_s$, $y_1(t)$ will approach zero with $y_{1_L}(t)$ without resaturating. Thus, with internal stability, no steady-state saturation, and $y_{1_L}(t)$ stable, $y_1(t) \to 0$ as $t \to \infty$. Of course, what has been demonstrated for $y_1(t)$ also holds for $y_2(t)$ with internal stability, no steady-state saturation, and $y_{2_L}(t)$ stable. All that remains to be proven is that each $y_{i_L}(t) \to 0$.

Proof that $y_{2_L}(t) \to 0$. First let $n_2 = 1.0$ but retain the nonlinear n_1. Call the $y_{1_L}(t)$ that would exist $y_{1_L}(t)|_{n_2=1}$. This would be the signal that would exist with a completely linear system. Since the linear system has been designed to be stable, $y_{1_L}(t)|_{n_2=1} \to 0$ as $t \to \infty$, as would the actual output of the nonlinear n_1, $y_1(t)$. Now with $y_1(t)$ out of saturation and approaching zero and with $n_2 = 1.0$, we have a linear system. Again since the linear system has been designed to be stable, $y_{2_L}(t) \to 0$ as $t \to \infty$. This is the $y_{i_L}(t)$ that can be used in a treatment identical to that of the preceding paragraph, which will show that, with both n_1 and n_2 nonlinear, $y_2(t) \to 0$ as $t \to \infty$.

Proof that $y_{1_L}(t) \to 0$. Repeat the proof above, beginning now with $n_1 = 1.0$ but retaining nonlinear n_2. The result will be that $y_{1_L}(t)$, and hence $y_1(t)$, approaches zero as $t \to \infty$, with both n_1 and n_2 nonlinear. It is again worth repeating that $y_{i_L}(t)$ represents the $y_i(t)$ that would exist if $n_i = 1.0$ but with the remaining nonlinearities in place.

The proof above can be extended to 3×3 systems, etc.

Design Summary

The details of the somewhat torturous analyses of the previous sections are not necessary for design. One begins with a stable linear design and creates the individual elements g'_{ij}, h_i through Eqs. (15) and (16) (or their scalar counterparts for nonsquare $\boldsymbol{P}$). Then one checks for internal stability and no steady-state saturation.

Example

The example to be considered here concerns command limiting in the longitudinal control system for a simple model of a rotorcraft. The rotorcraft dynamics, taken from Ref. 8, are given in the Appendix and correspond to trimmed level flight at 60 knots. The control system is shown in Fig. 5 and consists of an altitude and airspeed hold autopilot. The compensations g_θ, $g_{\dot{h}}$, g_u, and g_h are given in Table 1 with g_θ and $g_{\dot{h}}$ providing inner loop crossover frequencies of 5 rad/s. Note that, as opposed to Fig. 3a, the compensation matrix $\boldsymbol{G}$ of Fig. 5 is diagonal. Command limiting is shown in the outer loops of the control system of Fig. 5. Such limiting is common in flight control systems to prevent large vehicle upsets occurring when setpoint changes are commanded through the autopilot. For precise path and speed tracking, however, the limiting may cause performance degradation, which we wish to minimize with the design technique discussed herein.

Figure 6 shows the nonlinear design. The $L_{n_i}(s)$ for both nonlinearities was chosen as 50/s. Equations (15) and (16) can be used to determine the desired g'_{ij}. The absence of g_{ij} in the original design simplifies the equations significantly. With $\boldsymbol{P}''$ representing

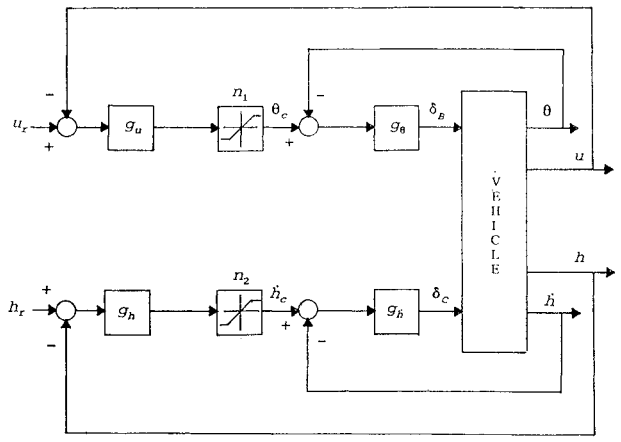

Fig. 5 Rotorcraft longitudinal flight control system with command limiting.

Table 1 Compensator transfer functions for Figs. 5 and 6

$$g_\theta = \frac{-11{,}145(0.45)^2(3)^{a}}{(0)^2(50)^2} \qquad g_u = \frac{-0.621(0.1)^2}{(0)^2(20)}$$

$$g_{\dot h} = \frac{19.91(0.45)}{(0)(50)} \qquad g_h = \frac{20(0.1)}{(0)(20)}$$

$$g'_{11} = \frac{-0.6211(10)^2(50)(0.1)^2(0.0338)}{(0)(17.73)(16.17)(4.69)(1.2)(0.15)(0.0821)}$$

$$g'_{22} = \frac{20(50)(4.72)(0.1)}{(20.49)(2.61)(1.58)(0.112)}$$

$$h_1 = \frac{50(19.45)(12.44)(8.11)(.0361)}{(17.73)(16.17)(4.69)(1.2)(0.15)(0.0821)}$$

$$h_2 = \frac{50(20.2)(4.59)(-0.0204)}{(20.49)(2.61)(1.58)(0.112)}$$

[a] $(\alpha) = s + \alpha$.

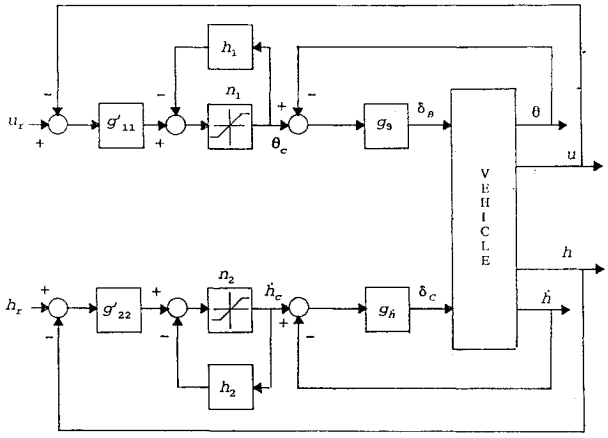

Fig. 6 Nonlinear design for system of Fig. 5.

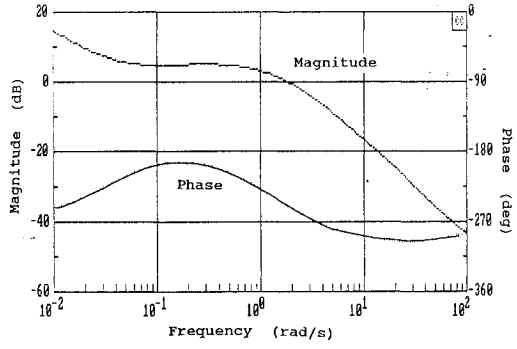

Fig. 7 Bode diagram for $g'_{11}(s)$ from system of Fig. 6.

the effective plant matrix with θ_c and $\dot h_c$ as inputs and u and h as outputs, one has

$$g'_{11} = \frac{1 + L_{n_1}}{1/g_u + P''_{11}} \qquad g'_{12} = g'_{21} = 0 \qquad g'_{22} = \frac{1 + L_{n_2}}{1/g_h + P''_{22}} \tag{23}$$

$$h_1 = L_{n_1} - P''_{11}g'_{11} \qquad h_2 = L_{n_2} - P''_{22}g'_{22}$$

The resulting g'_{ii} and h_i elements were of greater than 10th order but could be closely approximated by lower order fits. These fits are shown in Table 1. As an example of the nature of the g'_{ii} and h_i dynamics that result from the design, Figs. 7 and 8 show the Bode diagrams for g'_{11} and h_1 associated with the airspeed loop. The dynamics are quite reasonable, i.e., no amplitude magnification at high frequency.

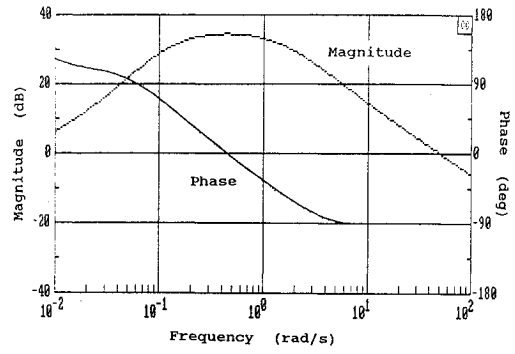

Fig. 8 Bode diagram for $h_1(s)$ from system of Fig. 6.

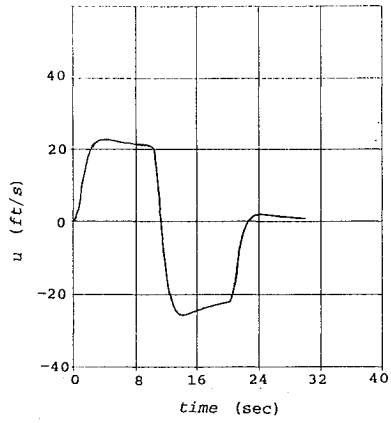

Fig. 9 Airspeed doublet response for system of Fig. 5 with no command limiting.

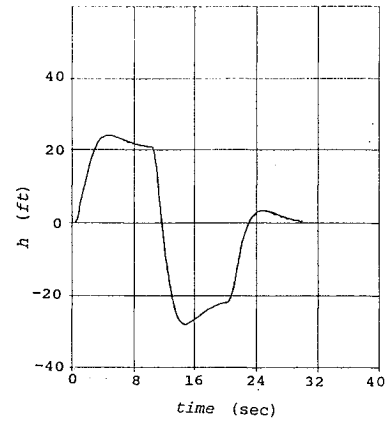

Fig. 10 Altitude doublet response for system of Fig. 5 with no command limiting.

The saturation levels of the command limiters in Figs. 5 and 6 were chosen as 0.15 rad and 10 ft/s. These values were selected to guarantee limiting behavior given the input commands u_r and h_r to be defined. The sufficient conditions for stability were met. Internal stability was in evidence, and Eq. (17) was satisfied for all possible combinations of limiting values.

The u_r and h_r transient commands were filtered doublets applied simultaneously. The duration of each doublet pulse was 10 s. The amplitudes were 20 ft/s and 20 ft for u_r and h_r, respectively. The filter was second order, with $\zeta = 1.0$ and $\omega_n = 5$ rad/s.

When simulated, longitudinal cyclic and collective actuator dynamics and actuator rate limiting (swashplate angular rate) were included in the model, as indicated in the Appendix. The purpose of these model additions was to demonstrate that any performance improvements that accrued with the nonlinear design were not accompanied by unrealistic control inputs to the basic airframe. The actuator dynamics, however, were not considered in the design of the compensators shown in Table 1.

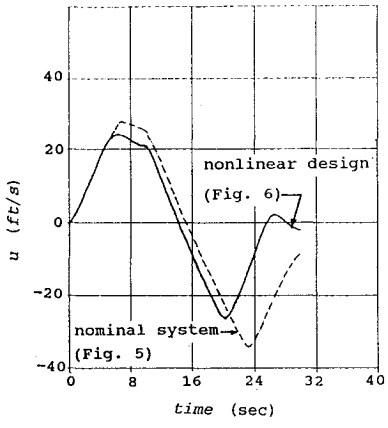

Fig. 11 Airspeed doublet responses for systems of nominal (Fig. 5) and nonlinear (Fig. 6) designs.

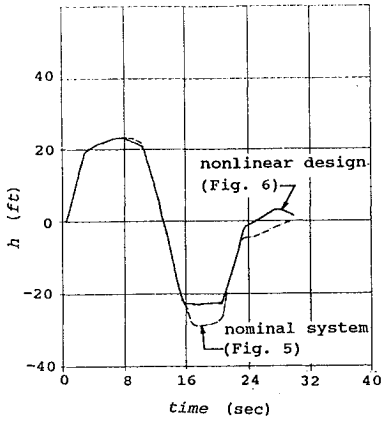

Fig. 12 Altitude doublet responses for systems of nominal (Fig. 5) and nonlinear (Fig. 6) designs.

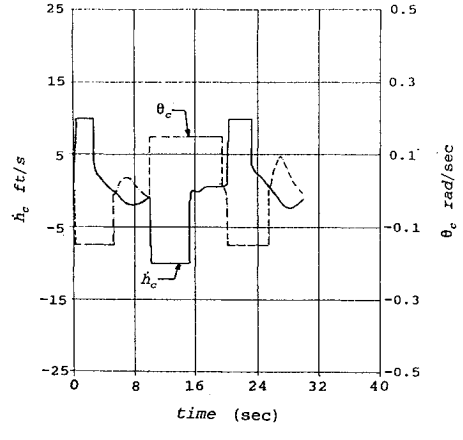

Fig. 13 Pitch attitude and altitude–rate command limiting in system of Fig. 6.

Figures 9 and 10 show the airspeed and altitude responses of the system with no command limiting. Figures 11 and 12 compare the responses of the original (nominal) and nonlinear designs, both with the command limiting. Note the improved performance of the nonlinear design, particularly in the airspeed response. Finally, Fig. 13 shows the command limiting that occurred in the simulation with the nonlinear design. Note the occurrence of significant and simultaneous saturation.

Discussion

As the authors of Refs. 3 and 4 point out, there has been little, if any, research that addresses and solves the integrator or reset windup problem[9] for MIMO systems. This issue has not been explicitly addressed in the design technique proposed in this study simply because the need to do so did not arise. The ability of $y_i(t)$ to approach $y_{i_L}(t)$ with dynamics $(1 + L_{n_i})^{-1}$ after $y_i(t)$ comes out of saturation is not predicated upon the absence of integrators before the nonlinearity. One might argue, of course, that some of the design restrictions that have been employed, e.g., transient inputs, and the constraints of Eqs. (17) and (19) simply reduce the impact of windup upon system performance.

Note that there would be no additional sensing requirements in implementing the system of Fig. 6 as compared to that of Fig. 5. The command limiting and creation of g'_{ii} and h_i could all be accomplished in software in the flight control computer. Finally, research is presently underway with the goal of eliminating the requirement for a stable plant and in ensuring that an internally stable design is created.

Conclusions

Based upon the preceding analyses and example, the following conclusions can be drawn:

1) A technique for improving the performance of a MIMO control system in the presence of saturating nonlinearities has been developed. The nonlinear design is derived entirely from a linear control system formulation.

2) Sufficient conditions for closed-loop stability have been presented including the necessity of a stable plant.

3) Although the analyses supporting performance improvements and stability were quite involved, the design equations themselves are simple to formulate and solve.

4) A means of determining whether the technique guarantees stability in individual compensation elements is currently being investigated.

5) One immediate application of the technique is in systems in which command limiting is part of the design requirements.

Appendix: Vehicle and Actuator Models

Vehicle model:

$$\dot{\boldsymbol{x}}(t) = \boldsymbol{A}\boldsymbol{x}(t) + \boldsymbol{B}\boldsymbol{u}(t)$$

$$\boldsymbol{y} = \boldsymbol{C}\boldsymbol{x}(t) \tag{A1}$$

$$\boldsymbol{x} = \{u, w, q, \theta\}^T \qquad \boldsymbol{u} = \{\delta_B, \delta_C\}^T$$

$$\boldsymbol{y} = \{u, \dot{h}\}^T$$

$$\boldsymbol{A} = \begin{bmatrix} -0.0338 & 0.0311 & 1.044 & -32.17 \\ -0.0564 & -0.7886 & 101.45 & -0.331 \\ 0.0179 & 0.0129 & -3.6151 & 0 \\ 0 & 0 & 1.0 & 0 \end{bmatrix}$$

$$\boldsymbol{B} = \begin{bmatrix} 0.5806 & 0.2462 \\ 1.483 & -17.798 \\ -0.8220 & 0.8031 \\ 0 & 0 \end{bmatrix} \tag{A2}$$

$$\boldsymbol{C} = \begin{bmatrix} 1 & 0 & 0 & 0 \\ 0 & -1 & 0 & 101.45 \end{bmatrix}$$

Actuator dynamics:

$$\frac{(25)^2}{s^2 + 2(0.707)(25)s + (25)^2} \tag{A3}$$

Actuator rate limit: 50 deg/s.

References

[1]Horowitz, I., *Quantitative Feedback Design Theory*, QFT Publications, Boulder, CO, 1993.

[2]Smith, G. A., and Meyer, G., "Aircraft Automatic Flight Control System with Model Inversion," *Journal of Guidance, Control, and Dynamics*, Vol. 10, No. 3, 1987, pp. 269–275.

[3]Kapasouris, P., Athans, M., and Stein, G., "Design of Feedback Control Systems for Stable Plants with Saturating Actuators," *Proceedings of the Twenty-Seventh Conference on Decision and Control* (Austin, TX), 1988, pp. 469–479.

[4]Kapasouris, P., Athans, M., and Stein, G., "Design of Feedback Control Systems for Unstable Plants with Saturating Actuators," *IFAC Symposium on Nonlinear Control Systems Design* (Capri, Italy), edited by A. Isidori, 1989, pp. 302–307.

[5]Horowitz, I., "A Synthesis Theory for a Class of Saturating Systems," *International Journal of Control*, Vol. 38, 1984, pp. 169–187.

[6]Horowitz, I., "Feedback Systems with Rate and Amplitude Limiting," *International Journal of Control*, Vol. 40, 1986, pp. 1215–1229.

[7]Hess, R. A., and Snell, S. A., "Feedback Design with Saturation Nonlinearities: Single-Input, Single-Output Systems with Unstable Plants," *Journal of Guidance, Control, and Dynamics* (submitted for publication).

[8]Jung, Y. C., and Hess, R. A., "Precise Flight-Path Control Using a Predictive Algorithm," *Journal of Guidance, Control, and Dynamics*, Vol. 14, No. 5, 1991, pp. 936–942.

[9]Astrom, K. J., and Wittenmark, B., *Adaptive Control*, Addison–Wesley, Reading, MA, 1989.